

Magnetophonon and electrophonon resonances in quantum wires

Sang Chil Lee, Young Bong Kang, Doo Chul Kim, and Jai Yon Ryu
Department of Physics, Cheju National University, Cheju 690-756, Republic of Korea

Nam Lyong Kang and Sang Don Choi
Department of Physics, Kyungpook National University, Taegu 702-701, Republic of Korea
 (Received 2 October 1996; revised manuscript received 20 November 1996)

Based on the formalism developed previously [Phys. Rev. B **48**, 9126 (1993)], magnetophonon resonances and electrophonon resonances in quantum wires are investigated for various confinement potentials. The occupation of several electric subbands due to these confinement potentials leads to electrophonon resonances and a splitting and shift of magnetophonon resonance peak positions. The dependence of both resonance peak positions on the magnetic field, the thickness of the well, the confinement frequency, and the bias field is shown explicitly. [S0163-1829(97)08711-0]

I. INTRODUCTION

Magnetophonon resonances (MPR's) and electrophonon resonances (EPR's) in low-dimensional electron gas systems have generated considerable interest in recent years. Many studies have been made on these effects in two-dimensional electron gas (2DEG) systems.¹⁻⁵ However, less work has been done on the effects of a quasi-one-dimensional electron gas (Q1DEG).⁶⁻⁸ Vasilopoulos *et al.*⁶ studied MPR effects in quantum wires assuming a parabolic confinement potential of frequency Ω , based on the Kubo formula⁹ and the quantum Boltzmann equation,² and their calculations revealed that the ordinary resonance condition $\omega_L = P\omega_c$ is modified to $\omega_L = P\tilde{\omega}_c$, where P is an integer, ω_L and ω_c are the LO-phonon frequency and cyclotron frequency, respectively, and $\tilde{\omega}_c$ is the renormalized cyclotron frequency given by $\tilde{\omega}_c = (\omega_c^2 + \Omega^2)^{1/2}$. Mori *et al.*⁷ presented a theory of MPR for the same model as treated by Vasilopoulos *et al.*⁶ by utilizing the Kubo formula and the Green's function method.¹⁰ A numerical analysis with respect to the magnetoconductivity has been performed for weak and strong confinement potentials by introducing the current density operator due to the electron-phonon interaction and the confinement potential. Recently, Ryu and O'Connell⁸ have presented a theory of MPR's for the same model as treated by Vasilopoulos *et al.*⁶ by taking the linear response limit of nonlinear response theory¹¹ in order to investigate analytically the MPR effects in quantum wires. It should be pointed out that they assumed that only the lowest subband level formed in the heterostructures is occupied. This assumption leads to the neglect of effects arising from a consequence of the occupation of several electric subbands such as EPR effects, the splitting of MPR peak positions, and the shift of MPR peaks. The purpose of the present paper is to study the MPR and EPR effects of a Q1DEG in quantum wires, where electric subbands are considered.

II. MODEL FOR QUANTUM WIRES

We consider a simple model for a quantum wire, in which a two-dimensional electron gas formed in heterostructures is

confined by narrow gates or split gates, and electrons are free along only one direction. We assume that a heterointerface is normal to the z axis and the confinement in the y direction is characterized by a parabolic potential of frequency Ω_y . For the confinement potentials along the z axis, we take the following potential wells: (1) the parabolic well and (2) the square well, which both have the advantage that all subbands can be included in the calculation, and (3) the triangular well, which is often used to model heterostructures. Applying a static magnetic field $\vec{B}(\parallel \hat{z})$ to the wire and considering the effective-mass approximation for conduction electrons confined in the quantum wire, the one-particle Hamiltonian (h_e) for such electrons together with its normalized eigenfunctions ($|\lambda\rangle$) and eigenvalues (E_λ), in the Landau gauge of vector potential $\vec{A} = (-By, 0, 0)$, are, respectively, given by

$$h_e = (\vec{p} - e\vec{A})^2/2m^* + m^*\Omega_y^2 y^2/2 + h(z), \quad (1)$$

$$|\lambda\rangle \equiv |N, n, k_x\rangle = \phi_N(y - y_\lambda) \exp(ik_x x) \Psi_n(z) / \sqrt{L_x}, \quad (2)$$

$$E_\lambda \equiv E_{N, n, k_x} = (N + 1/2)\hbar\tilde{\omega}_c + \hbar^2 k_x^2/2\tilde{m} + \varepsilon_n, \quad (3)$$

where \vec{p} is the momentum operator of a conduction electron, N ($= 0, 1, 2, \dots$) and n denote the Landau-level index and the subband-level index, respectively, and $\tilde{\omega}_c = (\omega_c^2 + \Omega_y^2)^{1/2}$ and $\tilde{m} = m^*\tilde{\omega}_c^2/\Omega_y^2$ are the renormalized cyclotron frequency with respect to the cyclotron frequency $\omega_c = eB/m^*$ and the renormalized mass with respect to the effective mass m^* associated with the characteristic frequency of the confinement potential Ω_y , respectively. Also $\phi_N(y - y_\lambda)$ represents harmonic-oscillator wave functions, centered at $y = y_\lambda = -\tilde{b}\tilde{l}_B^2 k_x$. Here k_x is the wave vector in the x direction, $\tilde{b} = \omega_c/\tilde{\omega}_c$, and $\tilde{l}_B = (\hbar/m^*\tilde{\omega}_c)^{1/2}$ is the effective radius of the ground-state electron orbit in the (x, y) plane. The dimensions of the sample are assumed to be $V = L_x L_y L_z$.

For a parabolic well given by $h(z) = m^*\Omega_z^2 z^2/2$ with the characteristic frequency of the confinement potential Ω_z , the eigenfunctions $\Psi_n(z)$ and the corresponding eigenvalues ε_n are, respectively, given by

$$\Psi_n(z) = (1/2^n \pi^{1/2} l_B n!)^{1/2} \exp(-z^2/2l_B^2) H_n(z/l_B), \quad (4)$$

$$\varepsilon_n = (n + \frac{1}{2}) \hbar \Omega_z, n = 0, 1, 2, \dots, \quad (5)$$

where $l_B = (\hbar/m^* \Omega_z)^{1/2}$.

For a square well of infinite height, the eigenfunctions and eigenvalues, respectively, are known to be

$$\Psi_n(z) = \sqrt{\frac{2}{L_z}} \sin\left(\frac{n\pi}{L_z} z\right), \quad (6)$$

$$\varepsilon_n = n^2 \varepsilon_0, \quad n = 1, 2, 3, \dots, \quad (7)$$

where $\varepsilon_0 = \hbar^2 \pi^2 / 2m^* L_z^2$.

For the half-triangular-well case given by $h(z) = eF_s z$ ($z > 0$), ∞ ($z < 0$), the eigenfunctions are given by Airy functions¹² as

$$\Psi_n(z) = Ai\left[\left(\frac{2m^* e F_s}{\hbar^2}\right)^{1/3} \left(z - \frac{\varepsilon_n}{e F_s}\right)\right], \quad (8)$$

where the eigenvalues are approximately given by

$$\varepsilon_n = \left(\frac{\hbar^2 e^2 F_s^2}{2m^*}\right)^{1/3} \left[3\pi \left(n + \frac{3}{4}\right)/2\right]^{2/3}, \quad n = 0, 1, 2, \dots \quad (9)$$

Here F_s is an applied bias field in the z direction of the heterostructure.

III. MAGNETOPHONON AND ELECTROPHONON RESONANCES

The transverse magnetoconductivity σ_{xx} for the Q1D version can be evaluated from the linear-response limit with respect to Eq. (4.38) of Ref. 11 given in the nonlinear-response theory, which is expressed by the sum of the hopping part σ_{xx}^h and the nonhopping part σ_{xx}^{nh} as⁸

$$\sigma_{xx}^h \approx (e^2 \tilde{b}^2 \tilde{l}_B^2 N_s^{1D} / \hbar^2 \tilde{\omega}_c V) \tilde{\Gamma}_{0\lambda+1\lambda}, \quad (10)$$

$$\sigma_{xx}^{nh} \approx (\hbar e^2 \tilde{\omega}_c^2 N_s^{1D} / m^* \Omega_y^2 V) [\tilde{\Gamma}_{0\lambda\lambda}]^{-1}, \quad (11)$$

where $N_s^{1D} = \sqrt{\tilde{m} L_x^2 / 8\pi \hbar^2 \beta} \sum_n \exp[\beta(E_F - \varepsilon_n)] / \sinh(\beta \hbar \tilde{\omega}_c / 2)$, with E_F being the Fermi energy, $\beta = 1/k_B T$, with k_B being Boltzmann's constant, $X_{\lambda\lambda'} \equiv \langle \lambda | X | \lambda' \rangle$ for any operator X , and $\tilde{\Gamma}_{0\lambda_2\lambda_1}$ is the relaxation rate associated with the states λ_1 and λ_2 . To obtain the above equations we have performed the sum over the λ state with the use of Eq. (2). Using Eqs. (2) and (3) and proceeding as in Ryu and O'Connell,⁸ the relaxation rates $\tilde{\Gamma}_{0\lambda+1\lambda}$ and $\tilde{\Gamma}_{0\lambda\lambda}$ are given as

$$\begin{aligned} \tilde{\Gamma}_{0\lambda+1,\lambda} &\approx \tilde{\Gamma}_{0\lambda,\lambda} \approx 2\pi(N_0 + 1/2 \pm 1/2) \sum_{\lambda' \neq \lambda} F_q(N, N'; n, n') \\ &\times \delta[(N' - N)\hbar \tilde{\omega}_c + \hbar \omega_{n',n} \pm \hbar \omega_L], \end{aligned} \quad (12)$$

with

$$F_q(N, N'; n, n') \equiv \sum_q |C(q)|^2 |J_{NN'}(u)|^2 |J_{nn'}(q_z)|^2, \quad (13)$$

where $\omega_{n',n} = (\varepsilon_{n'} - \varepsilon_n) / \hbar$, ω_L is the LO-phonon frequency, $C(q)$ is the interaction potential for LO-phonon scattering, N' indicates intermediate localized Landau states, N_0 is the LO-phonon distribution function given by $N_q^- = [\exp(\beta \hbar \omega_q^-) - 1]^{-1}$ with $\omega_q^- = \omega_L$, and

$$|J_{nn'}(\pm q_z)|^2 = \left| \int_{-\infty}^{\infty} \Psi_n^*(z) \exp(\pm i q_x z) \Psi_{n'}(z) dz \right|^2, \quad (14)$$

$$|J_{NN'}(u)|^2 = \frac{N_n!}{N_m!} e^{-u} u^{N_m - N_n} [L_{N_n}^{N_m - N_n}(u)]^2, \quad (15)$$

with $N_n = \min\{N, N'\}$, $N_m = \max\{N, N'\}$, $u = \tilde{l}_B^2 (\tilde{b}^2 q_x^2 + q_y^2) / 2$, and $L_N^M(u)$ being an associated Laguerre polynomial.¹³ In Eq. (12) we have made an approximation $N' \pm 1 \approx N'$ for very large N' and assumed that the phonons are dispersionless (i.e., $\hbar \omega_q^- \approx \hbar \omega_L \approx \text{const}$) and the system is of bulk (i.e., three dimensional). The energy-conserving δ functions in Eq. (12) imply that when the electron undergoes a collision by absorbing energy from the field, its energy can change only by an amount equal to the energy of a phonon involved in the transition. This in fact leads to the MPRs and/or EPR effects, for which $\hbar \tilde{\omega}_c$ and $\Delta \varepsilon_n \gg \tilde{\Gamma}_0$. The selection rule $\lambda' \neq \lambda$ in the summation of Eq. (12) means $(N', n') \neq (N, n)$, which contains the following conditions: (1) $N' \neq N$ and $n' = n$, (2) $N' = N$ and $n' \neq n$, and (3) $N' \neq N$ and $n' \neq n$. From these conditions, we can expect three possible transitions in quantum wires: (1) the transition due to the Landau levels for the y direction, (2) the transition due to the subband levels for the z direction, and (3) the transition due to both the Landau levels for the y direction and the subband levels for the z direction.

Setting $N' - N = -P$ in the emission term and $N' - N = P$ in the absorption term⁶ and considering Eqs. (10), (11), and (12), we see from the above condition that the transverse magnetoconductivity shows resonant behaviors: MPR's at $P \tilde{\omega}_c = \omega_L$ and at $P \tilde{\omega}_c = \omega_L^\pm$ (P is an integer) with $\omega_L^\pm = \omega_L \pm \omega_{n',n}$. Those resonances involving the terms $\omega_{n',n}$ reflect the subband structure in the z direction. The MPR condition at $P \tilde{\omega}_c = \omega_L$ is identical with those indicated by Vasilopoulos *et al.*⁶ Furthermore, we see from the above condition that the conductivity shows other resonant behaviors: EPR's due to the subband in the z direction at $\omega_{n',n} = \omega_L$. Note that, in the zero-magnetic-field case, the relaxation rate (and hence the electric conductivity) obtained by replacing $\tilde{\omega}_c$ in Eq. (12) by Ω_y , shows resonant behaviors: EPR's due to the subband level in the y direction at $P \Omega_y = \omega_L$ and at $P \Omega_y = \omega_L^\pm$ (P is an integer), and EPR's due to the subband in the z direction at $\omega_{n',n} = \omega_L$ and at $\omega_{n',n} = \omega_L \pm P \Omega_y$. In this case, we also see that the subband level for the y or z direction leads to the splitting of EPR's whenever virtual interelectric subband transitions take place.

Employing the collision-broadening model⁶ and applying Poisson's summation formula¹⁴ for the Σ_P in Eq. (12) we then obtain the relaxation rate for three different confinement potentials as

$$\begin{aligned} \tilde{\Gamma}_{0\lambda+1,\lambda} \approx \tilde{\Gamma}_{0\lambda,\lambda} \approx & \sqrt{\frac{2\pi\tilde{m}L_x^2}{\beta\hbar^3\omega_c}} (N_0 + 1/2 \pm 1/2) \sum_{n'} \operatorname{Re} \left\{ F_q \left(\frac{i\gamma_1}{\hbar\tilde{\omega}_c} + \frac{\omega_L^\pm}{\tilde{\omega}_c}; n, n' \right) \right\} \Psi \left(\frac{\gamma_1}{\hbar\tilde{\omega}_c}, \frac{\omega_L^\pm}{\tilde{\omega}_c} \right) \\ & + \sqrt{\frac{2\pi\tilde{m}L_x^2}{\beta\hbar^2}} (2N_0 + 1) S^{\text{osc}}(n; n'), \end{aligned} \quad (16)$$

where

$$S^{\text{osc}}(n; n') = \begin{cases} (1/\hbar\Omega_z) \operatorname{Re}\{F_q(N, N'; i\gamma_2/\hbar\Omega_z + \omega_L/\Omega_z)\} \Psi(\gamma_2/\hbar\Omega_z, \omega_L/\Omega_z) & \text{(parabolic well),} \\ [1/2\varepsilon_0(n+x_1)] \operatorname{Re}\{F_q(N, N'; i\gamma_3/\varepsilon_0 + x_1)\} \Psi(\gamma_3/\varepsilon_0, x_1) & \text{(square well),} \\ [3(x_2+n+\frac{3}{4})/2F_s] \operatorname{Re}\{F_q(N, N'; i\gamma_4/F_s + x_2)\} \Psi(\gamma_4/F_s, x_2), & \text{(triangular well),} \end{cases} \quad (17)$$

$$\Psi(a, b) = 1 + 2 \sum_{s=1}^{\infty} e^{-2\pi sa} \cos(2\pi sb) = \frac{\sinh(2\pi a)}{\cosh(2\pi a) - \cos(2\pi b)} \quad (a > 0), \quad (18)$$

with $x_1 = \sqrt{n^2 + \omega_L/\varepsilon_0} - n$, $x_2 = \sqrt{\{(n+3/4)^{2/3} + \omega_L/F_s\}^3 - (n+3/4)}$, and $\gamma_i (i=1,2,3,4)$ being the damping parameters.

IV. NUMERICAL RESULTS

To visualize the series of resonance positions associated with MPR and EPR effects in the quantum wires, we showed the plots in Figs. 1 and 2, where the optical-phonon energy has been taken as $\hbar\omega_L = 36.6$ meV for GaAs. Figure 1 shows the energy diagram of the MPR's at $P\tilde{\omega}_c = \omega_L$ and at $P\tilde{\omega}_c = \omega_L^\pm$, as a function of magnetic field. The quantum number of the Landau level is indicated for each line, depending on the value of Ω_y . The crossing points give the resonance magnetic fields, which depend on the strength of confinement in the z direction. We notice that the resonance magnetic field decreases as Ω_y increases. In the case where only intraelectric-virtual-subband transitions ($n \rightarrow n' = n$) take place, i.e., $\omega_{n'n} = 0$, there is no splitting of the MPR's. However, we can see that whenever the interelectric (nonresonant-)virtual-subband transitions take place for a rel-

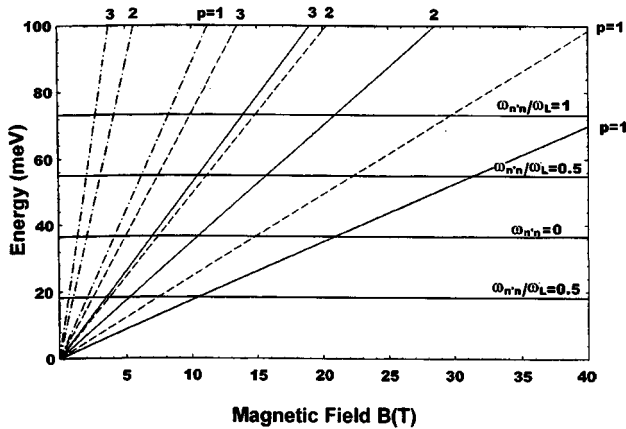


FIG. 1. Energy diagram is plotted as a function of magnetic field depending on the values of both characteristic frequency of the y -directional confinement and energy separation of the subbands for the z direction. The difference of the quantum number of the Landau level ($P=N'-N$) is indicated for each line. The solid, dotted, and dash-dotted lines are for $\Omega_y = 0.1\omega_c$, $\Omega_y = \omega_c$, and $\Omega_y = 5\omega_c$, respectively.

evant energy separation between subbands for the z direction, the splitting of the MPR peak positions occurs. The shift of the peak positions increases as the energy separation between two subband levels for the z direction increases.

Figures 2(a)–2(c) show the energy diagram of the EPR's at $\hbar\omega_{n'n} = \hbar\omega_L$ for three different confinement potentials for the z direction: a parabolic well, a square well, and a triangular well, respectively. The quantum number of the subband level in the z direction is indicated for each line, where the initial and final states are represented by n and n' , respectively. Any changes in the confinement frequency Ω_z , the well width L_z , and the bias field F_z lead to changes of the energy separation between electric subbands, which allow us to have the energy levels in resonance with the optical-phonon energy. The crossing points given in Figs. 2(a)–2(c) indicate the resonance confinement frequency, the resonance well width, and the resonance bias field, respectively. As can be seen from Fig. 2(a), no EPR takes place for $\Omega_z > 5.56 \times 10^{13} \text{ sec}^{-1}$ since the energy separation between adjacent subband levels is larger than the optical-phonon energy ($\hbar\omega_L = 36.6$ meV for GaAs). As Ω_z decreases (i.e., the well in z direction becomes wider), the energy separation between subbands n and n' becomes closer. Therefore, various resonance transitions from n to any n' are allowed to take place due to the LO phonons. Note that the reason for having the identical resonance frequencies for adjacent subband resonance transition is due to the fact that the energy separation between adjacent subband levels is all same. Unlike the parabolic well case, for the square well case given in Fig. 2(b), the resonance well widths for adjacent subband resonance transition have different values, which is due to the fact that every energy separation between adjacent subband levels is not the same because the subband energy spectrum ε_n is proportional to n^2 and is not equidistant. We can see that as the thickness of the well increases, various resonance transitions from the subband level n to any n' take place. The results for increasing the well width $L_z \sim 1/\sqrt{\Omega_z}$ are similar to those for decreasing the confinement frequency Ω_z in the parabolic potential case. For the triangular well case given in Fig. 2(c), the energy separation between adjacent subband levels is altered by changing the bias field

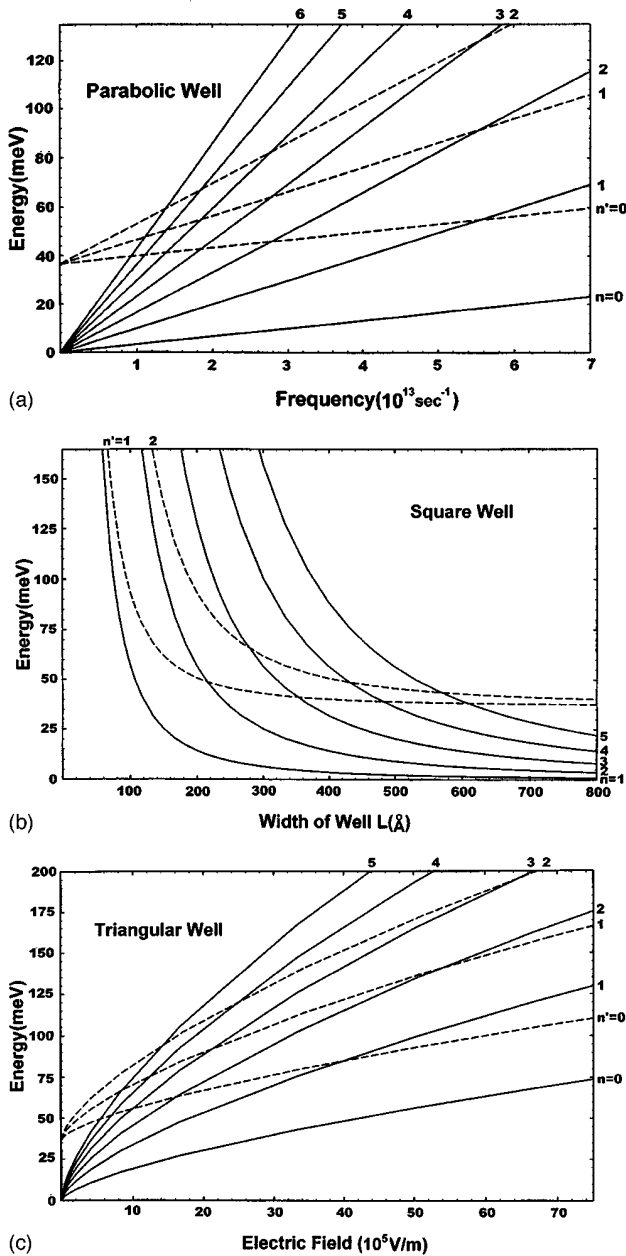


FIG. 2. Energy diagram is plotted as a function of (a) Ω_y , the characteristic frequency of the y -directional confinement for the parabolic well case, (b) L_z , the width of the well for the square well case, and (c) F_s , the electric field for the triangular well case. The quantum number of the subband level is indicated for each line.

F_z . As the bias field is increased the well width in the z direction is decreased. As a result, the energy separation between adjacent subband levels becomes larger. This is similar to the parabolic potential case because increasing the confinement frequency Ω_z is identical with decreasing the well width.

V. CONCLUSIONS

So far, we have studied MPR and EPR effects for a Q1D quantum-wire structure in the presence and absence of any magnetic field, in which a Q1DEG is confined by a parabolic well in the y direction and three kinds of confinement potentials in the z direction, including the parabolic well, the square well, and the triangular well. The relaxation rates (and hence the transverse magnetoconductivity) show resonant behaviors: MPR's at $P\bar{\omega}_c = \omega_L$ and at $P\bar{\omega}_c = \omega_L \pm \omega_{n'n}$ and EPR's due to the subband in the z direction at $\omega_{n'n} = \omega_L$, which strongly depends on the subband structure in the z direction. The occupation of several electric subbands gives rise to the additional oscillatory behavior of the MPR effect and EPR effect. It should be noted that the MPR peak positions are strongly sensitive to the strength of the magnetic field, the optical-phonon energy, the characteristic frequency of the y -directional confinement Ω_y , and the type of the confinement potential well in the z direction. The MPR condition at $P\bar{\omega}_c = \omega_L$ is identical to those of Vasilopoulos *et al.*,⁶ assuming that only the lowest subband level formed in heterostructures is occupied. In the zero magnetic-field case, the relaxation rates (and hence the electric conductivity) show resonant behaviors due to the subband levels given in two different directions: EPR's due to the subband level for the y direction at $P\Omega_y = \omega_L$ and at $P\Omega_y = \omega_L \pm \omega_{n'n}$, and EPR's due to the subband for the z direction at $\omega_{n'n} = \omega_L$ and at $\omega_{n'n} = \omega_L \pm P\Omega_y$.

In present calculation for the conductivity, we considered the most simple situation of linear transport and a nondegenerate electron gas. The nonlinear magnetophonon resonance and electrophonon resonance effects will be studied later.

ACKNOWLEDGMENTS

This research has been supported in part by the Basic Science Research Institute Program, Ministry of Education, under Grant No. BSRI-96-2405, and in part by the Korea Research Foundation, under Grant No. KRA427-95-01D0273.

¹R. J. Nicholas, Prog. Quantum Electron. **10**, 1 (1985).

²P. Vasilopoulos, Phys. Rev. B **33**, 8587 (1986).

³S. Komiyama, H. Eyferth, and J. P. Kotthaus, J. Phys. Soc. Jpn. **49**, Suppl. A, 687 (1980).

⁴A. Kastalsky *et al.*, Appl. Phys. Lett. **59**, 1708 (1991).

⁵W. Xu, F. M. Peeters, and J. T. Devreese, Phys. Rev. B **48**, 1562 (1993).

⁶P. Vasilopoulos *et al.*, Phys. Rev. B **40**, 1810 (1989).

⁷N. Mori, H. Momose, and C. Hamaguchi, Phys. Rev. B **45**, 4536 (1992).

⁸J. Y. Ryu, and R. F. O'Connell, Phys. Rev. B **48**, 9126 (1993).

⁹R. Kubo, J. Phys. Soc. Jpn. **12**, 570 (1957). G. D. Mahan, *Many-Particle Physics* (Plenum, New York, 1981).

¹⁰J. Y. Ryu and S. D. Choi, Phys. Rev. B **44**, 11 328 (1991).

¹¹*Handbook of Mathematical Functions*, edited by M. Abramowitz and I. A. Stegun, Natl. Bur. Stand. Appl. Math. Ser. No. 55 (U.S. GPO, Washington, D.C., 1964).

¹²I. S. Gradshteyn and I. M. Ryzhik, *Table of Integrals, Series, and Products* (Academic, New York, 1965).

¹³J. M. Ziman, *Principles of the Theory of Solids* (Cambridge University Press, Cambridge, England, 1972), p. 319.